therefore have lanthanum in X with p equal to 4 and sodium in M ($X^{[12-p]}$, $p = 6$). When two cations of different charges are present, the lower charged ion will preferentially occupy the Y polyhedron (La^{3+} in X, Na^+ in Y).

The average V–O distances in the four independent tetrahedra, 1.718, 1.700, 1.726, and 1.673 Å, respectively (Table II), are within the V–O distances reported recently by Robertson and Kostiner[12] in $FeVO_4$ (V–O = 1.660–1.806 Å) and by Gopal and Calvo[13] in $Ca_3(VO_4)_2$ (⟨V–O⟩ = 1.691, 1.701, and 1.694 Å for three independent tetrahedra). The average Na–O distances (Table II) fall into two categories: two short distances for Na(1) and Na(2)—2.408 and 2.437 Å, respectively—and four long distances for Na(3), Na(4), Na(5), and Na(6)—2.571, 2.586, 2.534, and 2.536 Å, respectively. These two different types of distances can be easily explained by the fact that the sodium atoms are present in two different sites. Atoms Na(1) and Na(2) are found in trigonal-antiprismal sites (octahedra) with very little cation–cation repulsion since the X polyhedra share faces only with other large X polyhedra. We have thus normal Na–O bonds. Sodium–oxygen bonds of similar length (2.418 Å) have been found by Durand et al.[14] in $K_3Na(PO_3F)_2$, where the sodium atom is in an equivalent position. Atoms Na(3) to Na(6) occupy the Y site, where there exists severe cation–cation repulsion between this polyhedron and the highly charged tetrahedron with which it shares a face. We can therefore expect much longer bonds.

The La–O distances all fall within values reported for $La_2Ti_2O_7$ (2.38–3.09 Å) by Gasperin[15] and for La_2MoO_6 (2.33–2.38 Å) by Sillén and Lundborg.[16] No La–La distances were found corresponding to significant bonding.

All O–O distances are normal with an average oxygen–oxygen distance of 2.800 Å. The individual O–V–O angles in the different tetrahedra are slightly distorted as expected, but the average tetrahedral angle of 109.4° is very normal.

In conclusion, in structures which are made up of isolated TX_4 tetrahedra, we observe that these tetrahedra can arrange themselves in a variety of ways by simply rotating around their centers and condensing themselves in "pinwheels" in such a way that they can accomodate in their network a number of different cations with different coordinations. This explains the fact that we find such compounds as β-K_2SO_4 and $K_3Na(PO_3F)_2$ to be topologically related.

Registry No. $Na_3La(VO_4)_2$, 55859-79-5.

Supplementary Material Available: A listing of structure factor amplitudes (17 pages). Ordering information is given on any current masthead page.

References and Notes

(1) J. A. Baglio and G. Gashurov, *Acta Crystallogr., Sect. B*, **24**, 292 (1968).
(2) E. Patscheke, H. Fuess, and G. Will, *Chem. Phys. Lett.*, **2**, 47 (1968).
(3) G. Blasse, and A. Brill, *Philips Tech. Rev.*, **31**, 324 (1970).
(4) G. Le Flem and R. Olazcuaga, *Bull. Soc. Chim. Fr.*, **7**, 2769 (1968).
(5) R. Salmon, C. Parent, A. Berrada, R. Brochu, A. Daoudi, M. Vlasse, and G. Le Flem, *C. R. Hebd. Seances Acad. Sci.*, **280**, 805 (1975).
(6) W. H. McMaster, N. Kerr del Grande, J. H. Mallet, and J. H. Hubbel, "Compilation of X-ray Cross Sections", Report UCRL-50174, National Bureau of Standards, 1969, Section II, Revision 1.
(7) D. T. Cromer, *Acta Crystallogr., Sect. B*, **18**, 17 (1965).
(8) P. B. Moore, and T. Araki, *Am. Mineral.*, **57**, 1355 (1972).
(9) P. B. Moore, *Am. Mineral.*, **58**, 32 (1973).
(10) B. Gossner, *Neues Jahrb. Mineral., Geol. Palaeontol., Abh. Abt. A*, **57**, 89 (1928).
(11) H. F. Fischmeister, *Monatsh. Chem.*, **93**, 420 (1962).
(12) B. Robertson and E. Kostiner, *J. Solid State Chem.*, **4**, 29 (1972).
(13) R. Gopal and C. Calvo, *Z. Kristallogr., Kristallgeom., Kristallphys., Kristallchem.*, **137**, 67 (1973).
(14) J. Durand, W. Granier, L. Cot, and J. L. Galigne, *Acta Crystallogr., Sect. B*, **31**, 1533 (1975).
(15) M. Gasperin, *Acta Crystallogr., Sect. B*, **31**, 2129 (1975).
(16) L. G. Sillén and K. Lundborg, *Z. Anorg. Chem.*, **252**, 2 (1943).

Contribution from the School of Chemistry, Rutgers University,
New Brunswick, New Jersey 08903

Crystal Structure and Magnetic Properties of Copper Citrate Dihydrate, $Cu_2C_6H_4O_7\cdot 2H_2O$

DONALD MASTROPAOLO, DANA A. POWERS, JOSEPH A. POTENZA,* and HARVEY J. SCHUGAR*

Received January 21, 1976 AIC60050M

The crystal and molecular structure of copper citrate dihydrate, $Cu_2C_6H_4O_7\cdot 2H_2O$, has been determined from single-crystal three-dimensional x-ray data collected by counter methods. The compound crystallizes as green six-sided plates in space group $P2_1/a$ (C_{2h}^5, No. 14) with $Z = 4$, $a = 14.477$ (9) Å, $b = 9.718$ (6) Å, $c = 6.890$ (5) Å, $\beta = 91.27$ (5)°, $d_{\text{calcd}} = 2.413$ g/cm^3, and $d_{\text{obsd}} = 2.39$ (1) g/cm^3. Least-squares refinement of 1172 reflections having $F^2 \geq 3\sigma$ gave a conventional R factor of 0.079. There are no discrete molecules in the crystal; it consists of a three-dimensional array of Cu(II) ions linked by alkoxo and three types of carboxylate bridges. The asymmetric unit contains two H_2O molecules, one heptadentate $C_6H_4O_7^{4-}$ citrate ligand, and two crystallographically unique Cu(II) ions with O_5 ligand sets. An alkoxo and a syn–syn carboxylate group bridge the Cu(II) ions within this unit. An anti–syn carboxylate group joins these units into zigzag chains, which in turn are joined by a second type of anti–syn carboxylate bridge to form the three-dimensional network. The complex does not exhibit the electronic absorption at ~380 nm which is characteristic of strongly coupled Cu(II) dimers. Its magnetism follows the Curie–Weiss law [$\chi \propto 1/(T-\Theta)$], with Θ falling in the +24–+40 K range. An unusual twisting of the Cu(II) coordination spheres within the asymmetric unit apparently suppresses the strong antiferromagnetism typically observed with alkoxo and syn–syn carboxylate bridged Cu(II) complexes.

The aqueous copper(II) citrate system has been studied extensively,[1] and several polynuclear species have been identified. A dimeric copper(II) citrate complex of possible composition $[Cu_2(OH)_2(C_6H_5O_7)_2]^{4-}$ has been characterized in solution, while, from a different sample, a Cu–Cu distance of 3.1 Å was deduced from a detailed ESR analysis.[1] Both magnetic susceptibility and ESR data indicated essentially no spin–spin coupling between Cu(II) ions. This result appeared odd to us at first because substantial antiferromagnetic interactions usually are observed between Cu(II) ions bridged presumably by ligands such as OH, alkoxo, and carboxylate (all available in the citrate system). However, recent studies of a series of $Cu_2(OH)_2^{2+}$ species have shown that the extent and nature of magnetic coupling (antiferromagnetic or fer-

Table I. Crystal Data for $Cu_2C_6H_4O_7 \cdot 2H_2O$

$Cu_2C_6H_4O_7 \cdot 2H_2O$	$d_{obsd} = 2.39(1)$ g/cm^3
Space group $P2_1/a$ (C_{2h}^5, No. 14)	$d_{calcd} = 2.413$ g/cm^3
$Z = 4$	$V = 969.1$ Å^3
$a = 14.477$ (9) Å	λ 0.710 69 Å
$b = 9.718$ (6) Å	$\mu = 45.6$ cm^{-1}
$c = 6.890$ (5) Å	$T = 22 \pm 1$ °C
$\beta = 91.27$ (5)°	

romagnetic) vary systematically with the Cu–OH–Cu bridging angle[2] and may in fact vanish at an angle of ~98°.

To determine if the magnetic peculiarity of the aqueous copper(II) citrate complex also exists in the solid state, we prepared $Cu_2cit \cdot 2H_2O$ (water insoluble) (cit = citrate) as a pure crystalline phase; it obeyed the Curie–Weiss law ($\mu = 1.80 \pm 0.07\ \mu_B$; $\Theta \simeq 30$ K) over the 85–300 K temperature range. This complex was prepared previously by Parry and DuBois.[3] On the basis of acidity measurements, they suggested that, even at pH ≤3, citrate could bind to Cu(II) as a $C_6H_4O_7^{4-}$ species in which the hydroxyl group as well as the three carboxyl groups are ionized. Their proposal of a highly condensed polymeric structure for this complex includes extensive ligand bridging of the Cu(II) ions. To help ascertain the structural basis of our magnetochemical results, we have determined the crystal structure of $Cu_2C_6H_4O_7 \cdot 2H_2O$.

Experimental Section

Preparation of $Cu_2C_6H_4O_7 \cdot 2H_2O$. Crystals of the water-insoluble complex were prepared by the urea hydrolysis technique. In a typical experiment, 4.20 g of citric acid dihydrate (0.02 mol), 3.41 g of $CuCl_2 \cdot 2H_2O$ (0.02 mol), and 2.40 g of urea (0.04 mol) were dissolved in 100 ml of distilled water. The resulting light blue solution was filtered through a Millipore membrane (0.22-μ pore size) and heated in an oven at 85 °C for 19 h. The green crystalline product was separated from the blue solution (pH 4.0) by decantation, thoroughly washed with distilled water, and air-dried (yield 3.2 g or 90% based on Cu). The product crystallized as six-sided elongated plates that exhibited a blue–green dichroism and extinctions that varied from complete to partial.

Anal. Calcd for $Cu_2C_6H_8O_9$: Cu, 36.18; C, 20.52; H, 2.30. Found: Cu, 36.0 (iodometry); C, 20.36; H, 2.03.

Microscopic examinations, ir spectral studies over the 4000–200-cm^{-1} spectral region, and density measurements indicated that the same product was obtained from reaction mixtures in which the ratio of Cu(II) to citric acid was varied from 2.0 to 0.5. Initial crystallization was observed at pH values as low as 1.9. $Cu_2cit \cdot 2D_2O$ was prepared by repeating the above procedure at $^1/_{10}$th scale with D_2O solvent and reagents that were previously exchanged with D_2O.

Magnetic Measurements. Variable-temperature magnetic susceptibility studies were performed in the laboratory of Professor Harry B. Gray with a PAR FM-1 vibrating-sample magnetometer; the apparatus and techniques used to collect the data have been described elsewhere.[4] A diamagnetic correction of 176 × 10^{-6} cgsu/Cu(II) was calculated from Pascal's constants.[5]

Collection of Diffraction Data. We were not able to obtain large crystals whose extinctions were sharp. Consequently, a relatively small crystal of dimensions 0.27 × 0.09 × 0.03 mm was mounted on the end of a glass rod parallel to the long dimension (b). Preliminary Weissenberg photographs showed systematic absences of $0k0$, $k = 2n + 1$, and $h0l$, $h = 2n + 1$, fixing the space group uniquely as $P2_1/a$. Unit cell dimensions (Table I) were determined from a least-squares analysis of the Θ, χ, and φ values of 11 reflections obtained using graphite-monochromated Mo Kα radiation (λ 0.71069 Å) and an Enraf-Nonius CAD-3 automated diffractometer. The crystal density was measured by the density gradient method using a mixture of tetrabromoethane and $CHCl_3$ as the high-density medium and $CHCl_3$ as the low-density medium.[6] NH_4Br ($d = 2.429$ g/cm^3) and KH_2PO_4 ($d = 2.338$ g/cm^3) were used as standards.[7] The observed density of 2.39 (1) g/cm^3 agreed well with the value of 2.413 g/cm^3 calculated for four $Cu_2C_6H_4O_7 \cdot 2H_2O$ units per unit cell.

A total of 3100 reflections were collected at room temperature (22 ± 1 °C). Graphite-monochromated Mo Kα radiation was detected with a scintillation counter and pulse height analyzer set to admit approximately 95% of the Kα peak. A θ–2θ scan was used to collect a unique data set in the range $1° \le \theta \le 30°$. Background measurements were made at the beginning and end of each scan with the counter stationary; the total time for background counting was equal to the scan time. The scan rate was $^1/_6$° s^{-1}, and each reflection was scanned repeatedly to a maximum of 10 scans or until 8000 total counts were obtained. Intensities were placed on a common scale by dividing by the number of scans. The intensity of one standard reflection, measured at 50-reflection intervals, was consistent to ±2%. Lorentz and polarization factors were applied to the 3100 measured intensities. Of these, 1172 with $F^2 \ge 3\sigma(F^2)$ were used in the structure solution and refinement. Here, $\sigma(F^2) = (Lp)^{-1}(N_t + (0.02N_n)^2)^{1/2}$ is the standard deviation as estimated from counting statistics, where N_t is the total count (background plus scan), N_n is the net count (scan minus background), and 0.02 is an estimate of instrumental instability. Absorption corrections were not considered necessary for the above crystal. The linear absorption coefficient for Mo Kα radiation was 45.6 cm^{-1} while maximum and minimum absorption factors for the data collected were calculated to be 1.46 and 1.17, respectively.

Solution and Refinement of the Structure.[8] The structure was solved by the heavy-atom method. There was some difficulty in locating the unique copper atoms from the Patterson map since one Cu happened to be very close to the glide plane at $y = ^1/_4$, and its $2x$, $2y$, $2z$ peak overlapped other vectors on the Harker plane at $v = ^1/_2$. However, approximate coordinates for the copper atoms were obtained from the normal sharpened Patterson map. Carbon and oxygen atoms were deduced from a difference synthesis based on the heavy-atom phases.

Initial refinement was based on F^2. Atomic scattering factors were those of Cromer and Waber[9] except for hydrogen scattering factors; these were obtained from ref 10. All atoms were treated as neutral species. Four cycles of refinement using isotropic temperature factors gave values of 0.14 and 0.23 for the functions $R_F = \sum||F_o| - |F_c||/\sum|F_o|$ and $R_{wF^2} = [\sum w(F_o^2 - F_c^2)^2/\sum wF_o^4]^{1/2}$, respectively; weights were set according to $w = 1/\sigma^2(F^2)$. All atoms were then allowed to vibrate anisotropically, and both real and imaginary parts of the anomalous dispersion corrections were applied to the copper atoms.[10] Two cycles of refinement reduced R_F and R_{wF^2} to 0.096 and 0.15, respectively.

Further refinement was based on F, and a weighting scheme was chosen by an analysis of variance to make $\Delta F/\sigma(F_o)$ independent of F_o. This led to the following assignments for $\sigma(F_o)$: $\sigma(F_o) = -0.12|F_o| + 1.84$ for $|F_o| \le 10.0$; $\sigma(F_o) = 0.64$ for $10.0 < |F_o| \le 18.6$; $\sigma(F_o) = 0.067|F_o| - 0.61$ for $|F_o| > 18.6$.

Attempts to locate hydrogen atoms were unsuccessful, and the coordinates of the four hydrogen atoms of the methylene carbons were calculated based on ideal tetrahedral geometry. A C–H bond distance of 1.08 Å was assumed and the isotropic temperature factor of each H atom was set equal to that of the attached carbon atom.

Three refinement cycles of all nonhydrogen positions and anisotropic temperature factors gave final values of 0.079 and 0.080 for R_F and R_{wF}, respectively. For the last cycle, all parameter changes were less than 0.1σ, where σ is the estimated standard deviation obtained from the inverse matrix. A final difference map showed a general background of approximately 0.5 e/Å^3 and revealed no significant features. Final atomic parameters, together with estimated standard deviations, are given in Table II while important interatomic distances and angles are presented in Table III. A view of the structure along the b axis is shown in Figure 1, and the unit cell contents are shown in Figure 2. A list of observed and calculated structure factors is available.[11]

Description of the Structure

The asymmetric unit (unprimed atoms in Figure 1) contains two crystallographically unique Cu(II) ions, one heptadentate $C_6H_4O_7^{4-}$ ligand, and two ligand H_2O molecules. Bridging of the Cu(II) ions by the alkoxide ion O(7), as well as by all three carboxylate groups, creates a three-dimensional network. Within the asymmetric unit, Cu(II) ions are separated by a distance of 3.242 Å. They are linked by a bent, symmetrical alkoxo bridge [Cu(1)–O(7)–Cu(2) = 115.2°; Cu(1)–O(7) = 1.925 Å; Cu(2)–O(7) = 1.916 Å] and by a carboxylate group from a neighboring citrate ligand. The carboxylate ligation in this bridge has an approximately syn–syn configuration, with Cu(1) lying 0.56 Å below the essentially planar arrangement of the Cu(2)–O(3′)–C(5′)–O(4′) fragment (Table IV). The

Table II.[a] Fractional Atomic Coordinates ($\times 10^4$) and Thermal Parameters[b]

Atom	x	y	z	β_{11} or B, Å^2	β_{22}	β_{33}	β_{12}	β_{13}	β_{23}
Cu(1)	−3375 (1)	7 522 (2)	1980 (2)	13 (1)	40 (1)	62 (3)	3 (1)	0 (1)	−16 (3)
Cu(2)	−1465 (1)	8 482 (2)	4122 (4)	14 (1)	95 (3)	274 (6)	−15 (1)	32 (2)	−114 (3)
O(1)	472 (6)	7 009 (10)	618 (15)	9 (4)	67 (12)	113 (21)	−2 (5)	−1 (8)	−4 (13)
O(2)	−369 (7)	8 147 (12)	2681 (18)	20 (5)	80 (14)	241 (33)	−16 (7)	12 (11)	−61 (18)
O(3)	−2564 (7)	4 061 (14)	4224 (17)	15 (4)	163 (16)	241 (33)	0 (8)	17 (9)	164 (20)
O(4)	−1285 (8)	3 784 (14)	5992 (16)	38 (6)	137 (18)	114 (26)	−25 (9)	−22 (10)	88 (17)
O(5)	−3286 (6)	5 850 (11)	534 (15)	9 (4)	64 (11)	121 (22)	4 (6)	−9 (8)	−57 (14)
O(6)	−2335 (7)	4 166 (12)	−192 (18)	29 (6)	64 (13)	231 (32)	3 (7)	23 (11)	−66 (18)
O(7)	−2188 (5)	7 002 (9)	3055 (13)	3 (3)	30 (9)	70 (18)	6 (5)	−9 (7)	−8 (11)
O(8)	−1300 (8)	10 755 (13)	3353 (16)	34 (6)	97 (15)	108 (24)	9 (8)	−23 (10)	−13 (17)
O(9)	−626 (8)	8 854 (13)	6584 (17)	27 (5)	106 (17)	131 (26)	0 (8)	−6 (9)	10 (17)
C(1)	−300 (9)	7 303 (12)	1274 (19)	19 (5)	4 (15)	84 (25)	−1 (7)	−2 (10)	14 (15)
C(2)	−1118 (9)	6 669 (15)	367 (20)	15 (5)	40 (15)	63 (25)	3 (8)	−8 (10)	−17 (17)
C(3)	−1743 (8)	5 973 (13)	1826 (20)	12 (5)	14 (12)	92 (28)	6 (7)	6 (10)	−27 (16)
C(4)	−1161 (9)	4 987 (17)	3089 (20)	12 (5)	71 (17)	63 (27)	6 (8)	21 (9)	26 (19)
C(5)	−1725 (8)	4 243 (13)	4546 (19)	13 (5)	2 (11)	87 (27)	2 (6)	15 (9)	−2 (15)
C(6)	−2487 (9)	5 237 (14)	683 (23)	10 (5)	27 (13)	131 (31)	−13 (7)	−1 (11)	−22 (17)
H(1)	−1523	7 485	−349	4.75					
H(2)	−906	5 937	−691	4.75					
H(3)	−622	5 564	3855	5.45					
H(4)	−845	4 225	2174	5.45					

[a] In this and in subsequent tables, numbers in parentheses are estimated standard deviations in the least significant digits. [b] Anisotropic thermal parameters are all $\times 10^4$ and are of the form $\exp[-(\beta_{11}h^2 + \beta_{22}k^2 + \beta_{33}l^2 + 2\beta_{12}hk + 2\beta_{13}hl + 2\beta_{23}kl)]$.

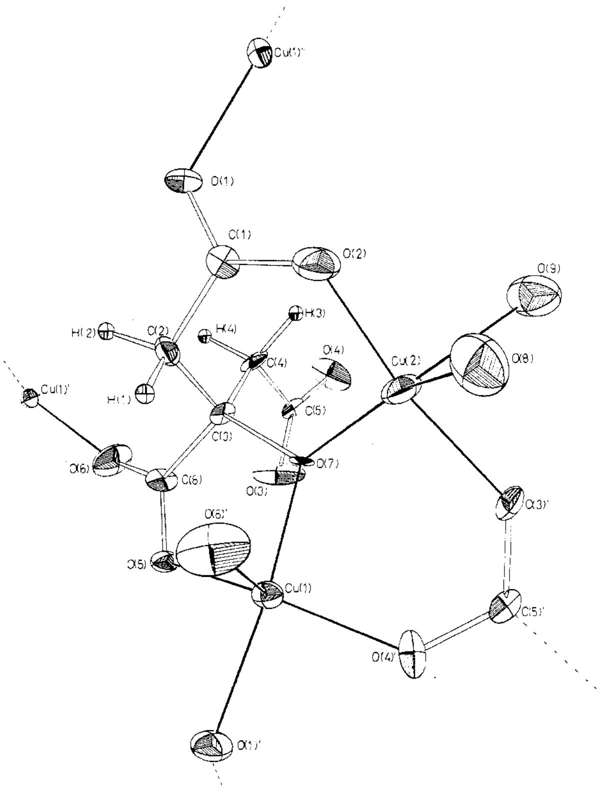

Figure 1. Perspective drawing of the $Cu_2cit\cdot 2H_2O$ unit indicating the intra- and interchain carboxylate bridging.

a-glide operation and the *a* unit cell translation give rise to a zigzag chain of Cu(II) ions in which Cu(2) and Cu(1'') of adjacent asymmetric units are linked by carboxylate group O(2)–C(1)–O(1). The carboxylate ligation in this Cu(2)–O(2)–C(1)–O(1)–Cu(1'') unit has an anti–syn configuration. The atoms in this unit deviate from planarity by as much as 0.21 Å with the carboxylate oxygen atoms showing the largest effect.

Finally, Cu(II) ions in different chains are related by the 2_1 screw axis along *b* and by unit cell translations along *c*. Linkage of the zigzag chains is established in two ways. The first manner (vide supra) involves the O(4)–C(5)–O(3) carboxylate associated with a given asymmetric unit serving as a syn–syn bridge between the Cu(II) ions in an adjacent unit. Another type of interchain linkage results from the third (and final) mode of carboxylate bridging and is restricted to the Cu(1) species. The carboxylate ligation in these Cu(1)–O(5)–C(6)–O(6)–Cu(1') interchain units has an anti–syn configuration. This unit shows deviations from planarity as large as 0.46 Å; thus, these atoms are considerably less coplanar than those of the Cu(2)–O(2)–C(1)–O(1)–Cu(1'') anti–syn unit.

Each copper atom is ligated by five oxygen donors. For Cu(1), the coordination geometry is approximately square pyramidal with the Cu(1)–O(6') bond apical. As expected, the apical Cu(1)–O(6') bond length (2.277 Å) is approximately 0.3 Å longer than each of the four equatorial Cu(1)–O bonds (1.912–1.952 Å). Cu(1) is displaced 0.14 Å from the least-squares basal plane defined by the carboxylate oxygen atoms O(1'), O(4'), and O(5) and the alkoxide oxygen atom O(7). Cu(1) is displaced toward O(6'), a carboxylate oxygen atom from a neighboring citrate molecule. In the approximately planar (±0.2 Å) basal oxygen unit, O–Cu(1)–O bond angles fall in the range 84.7–97.4°.

The coordination polyhedron of Cu(2) is more difficult to describe simply. Cu(2) has, as nearest neighbors, two H_2O oxygen atoms [O(8), O(9)], two carboxylate oxygen atoms [O(2), O(3')], and the bridging alkoxide oxygen atom [O(7)]. The Cu(2)–O(carboxylate) and Cu(2)–O(alkoxide) distances compare favorably with the corresponding distances for the equatorial atoms in the Cu(1) coordination sphere. Thus, on the basis of these distances, it is tempting to regard O(2), O(3'), and O(7) as equatorial. Similarly, since the Cu(2)–O(8) distance is approximately 0.19 Å longer than Cu(2)–O(9), O(8) might be regarded as apical and the coordination geometry as distorted square pyramidal. However, the "apical–equatorial" angle O(7)–Cu(2)–O(8) [134.1°] is too large to permit such a description. An alternative description of the coordination geometry is distorted trigonal bipyramidal with O(2) and O(3') apical [O(2)–Cu(2)–O(3') = 170.1°]. The sum of the angles involving Cu(2) and the "equatorial" atoms O(7), O(8), and O(9) [359.7°] supports such an interpretation. However, a trigonal-bipyramidal description offers no explanation for the difference in Cu(2)–OH_2 bond lengths. The true geometry lies between these extremes.

We note that the temperature factors for Cu(2) are considerably larger than those for Cu(1). This is consistent with

Table III. Bond Lengths (Å) and Bond Angles (deg)

Copper Coordination Spheres

Lengths

Cu(1)-O(1′)	1.952 (10)	Cu(2)-O(2)	1.918 (11)
Cu(1)-O(4′)	1.931 (9)	Cu(2)-O(3′)	1.914 (10)
Cu(1)-O(5)	1.912 (11)	Cu(2)-O(7)	1.916 (8)
Cu(1)-O(6′)	2.277 (11)	Cu(2)-O(8)	2.284 (11)
Cu(1)-O(7)	1.925 (8)	Cu(2)-O(9)	2.096 (11)
Cu(1)···Cu(2)	3.242 (6)		

Angles

O(1′)-Cu(1)-O(4′)	88.3 (4)	O(2)-Cu(2)-O(3′)	170.1 (6)
O(1′)-Cu(1)-O(5)	90.9 (4)	O(2)-Cu(2)-O(7)	97.2 (4)
O(1′)-Cu(1)-O(6′)	88.1 (4)	O(2)-Cu(2)-O(8)	87.2 (4)
O(1′)-Cu(1)-O(7)	173.8 (6)	O(2)-Cu(2)-O(9)	88.7 (4)
O(4′)-Cu(1)-O(5)	159.7 (6)	O(3′)-Cu(2)-O(7)	92.7 (4)
O(4′)-Cu(1)-O(6′)	94.1 (4)	O(3′)-Cu(2)-O(8)	86.3 (4)
O(4′)-Cu(1)-O(7)	97.4 (5)	O(3′)-Cu(2)-O(9)	83.5 (4)
O(5)-Cu(1)-O(6′)	106.1 (5)	O(7)-Cu(2)-O(8)	134.1 (5)
O(5)-Cu(1)-O(7)	84.7 (4)	O(7)-Cu(2)-O(9)	137.9 (5)
O(6′)-Cu(1)-O(7)	89.0 (4)	O(8)-Cu(2)-O(9)	87.7 (4)
Cu(1)-O(7)-Cu(2)	115.2 (1)		

Citrate Ligand

Lengths

C(1)-O(1)	1.25 (2)	C(2)-C(3)	1.52 (2)
C(1)-O(2)	1.28 (2)	C(3)-C(4)	1.53 (2)
C(5)-O(3)	1.24 (2)	C(3)-C(6)	1.50 (2)
C(5)-O(4)	1.25 (2)	C(4)-C(5)	1.49 (2)
C(6)-O(5)	1.30 (2)	C(2)-H(1)	1.07
C(6)-O(6)	1.23 (2)	C(2)-H(2)	1.09
C(3)-O(7)	1.47 (2)	C(4)-H(3)	1.09
C(1)-C(2)	1.46 (2)	C(4)-H(4)	1.08

Angles

O(1)-C(1)-O(2)	120 (1)	C(3)-O(7)-Cu(1)	110.9 (7)
O(1)-C(1)-C(2)	118 (1)	C(3)-O(7)-Cu(2)	119.2 (7)
O(2)-C(1)-C(2)	121 (1)	C(4)-C(3)-O(7)	110 (1)
O(3)-C(5)-O(4)	125 (1)	C(6)-C(3)-O(7)	108 (1)
O(3)-C(5)-C(4)	119 (1)	C(2)-C(3)-O(7)	111 (1)
O(4)-C(5)-C(4)	115 (1)	C(1)-C(2)-C(3)	113 (1)
O(5)-C(6)-O(6)	121 (1)	C(2)-C(3)-C(4)	109 (1)
O(5)-C(6)-C(3)	117 (1)	C(2)-C(3)-C(6)	107 (1)
O(6)-C(6)-C(3)	122 (1)	C(3)-C(4)-C(5)	112 (1)

Hydrogen-Bonding Distances[a]

$\mathrm{O(8)}_{5551}\cdots\mathrm{O(5)}_{4553}$	2.73
$\mathrm{O(8)}_{5551}\cdots\mathrm{O(9)}_{5762}$	2.81
$\mathrm{O(9)}_{5551}\cdots\mathrm{O(3)}_{4662}$	2.67
$\mathrm{O(9)}_{5551}\cdots\mathrm{O(2)}_{4454}$	2.81

[a] The first three subscripted integers represent unit cell translations along the *a*, *b*, and *c* crystallographic axes analogous to the ORTEP scheme and the last digit gives the symmetry operation according to: $1 = xyz$; $2 = \bar{x}\bar{y}\bar{z}$; $3 = {}^1/_2 - x, {}^1/_2 + y, \bar{z}$; $4 = {}^1/_2 + x, {}^1/_2 - y, z$.

the local environment of the two atoms. The Cu(1) atoms are coordinated only to oxygen atoms which form part of the rigid network; their amplitude of vibration is consequently expected to be small. In contrast, the Cu(2) atoms are each coordinated to two water molecules. They are therefore in a less rigid environment. This would lead to a larger amplitude of vibration.

The conclusion that deprotonation (required for charge balance) has occurred at O(7) instead of O(8) or O(9) cannot be drawn from the observed bond distances and angles within the Cu(II) coordination spheres. We could not locate H atoms nor discover precedents for identifying this deprotonation site directly from the observed structural parameters. The literature does contain numerous examples of Cu(II) ions bridged by RO^- or OH^- groups. We know of only one example of a bridging H_2O group,[12] while bridging of Cu(II) by ROH apparently is without precedent. Our formulation of O(8) and O(9) as ligand water molecules is supported by hydrogen-bonding distances (Table III) and by ir analysis. The possession of two hydrogen atoms by O(9) is required for hydrogen bonding to carboxylate oxygens O(3) and O(2). Two additional hydrogen atoms are required for the hydrogen bonding of O(8) to O(9) and the carboxylate oxygen O(5). The presence of ligand OH is also revealed by its characteristic infrared mode in the 1200–900-cm^{-1} spectral region.[13] Deformation modes of ligand H_2O are well removed toward lower energies.[13] The infrared spectra of $Cu_2cit\cdot 2H_2O$ and $Cu_2cit\cdot 2D_2O$ were identical over this range and support the chemically reasonable assignments of O(7) as alkoxide and O(8) and O(9) as ligand H_2O. The presence of ligand OH would require at least one of the infrared bands in this region to vanish upon isotopic substitution.

A consideration of special interest is the relative orientation of the Cu(1) and Cu(2) coordination spheres. This orientation, viewed from two different perspectives, is shown in Figures 1 and 3. It differs from the simple edge-shared arrangement observed for $Cu_2(OH)_2^{2+}$ units in two ways. First, substitution of the three-atom carboxylate bridge for one hydroxo bridge causes the Cu(1), O(1′), O(5), O(7), O(4′) and Cu(2), O(7), O(2), O(9), O(3′) planes to pivot about the alkoxide oxygen O(7). Second, the above planes are twisted from an idealized coplanar arrangement. The extent of twisting may be gauged by the dihedral angle between these planes (38.3°).

Structural parameters for the $C_6H_4O_7^{4-}$ ligand are comparable to those reported for $C_6H_5O_7^{3-}$ [14,15] and $C_6H_6O_7^{2-}$ [16] and will not be considered further.

Discussion

The structure of the title complex is, except for several details, the type of highly condensed network suggested by Parry and DuBois. Their formulation of the complex as $Cu_2C_6H_4O_7\cdot 2H_2O$ instead of $Cu_2(OH)C_6H_5O_7\cdot H_2O$ has proved to be correct.

We examine the observed magnetic susceptibility of this complex in light of those structural features which may allow spin–spin coupling of the Cu(II) ions. Three types of ligand-bridged Cu(II) ions are found in the title complex: (A) Cu(1) and Cu(2) linked within the asymmetric unit via an alkoxo and an approximately syn–syn carboxylate bridge; (B) Cu(2) and Cu(1″) linked by an anti–syn carboxylate bridge which joins the asymmetric units in a zigzag chain; (C) adjacent Cu(1) species linked by an anti–syn carboxylate bridge which serves to couple the chains into a three-dimensional network.

Magnetic susceptibility data over the 85–300 K temperature range have been obtained for three different preparations of $Cu_2cit\cdot 2H_2O$ (Table V). Plots of $1/\chi_M$ vs. T (not shown) revealed Curie–Weiss behavior. The Weiss temperatures of samples I and III were 25 ± 4 and 24 ± 4 K, respectively. A somewhat larger Weiss temperature of 40 ± 4 K was observed for sample II. We adopt the convention $\chi \propto 1/(T - \Theta)$; i.e., intersection of the T axis occurred in the +24–+40 K range. Thus, the net magnetic interaction between the Cu(II) ions is small. The magnetic moments ($\mu = (7.998\chi_M T)^{1/2}$) of I and III increased about 0.2 μ_B upon cooling from ~300 to ~90 K. For reasons not yet understood, the magnetic moment of sample II also increased by ~0.2 μ_B but achieved a maximum value at ~150 K. After the magnetic interactions were corrected using the Curie–Weiss relationship, all three samples exhibited an essentially temperature-independent apparent magnetic moment, defined as $\mu_{CW} = [7.998\chi_M(T - \Theta)]^{1/2}$, in the 1.75–1.83-$\mu_B$ range. Some type of spin–spin coupling was further evidenced by our inability to detect ESR absorption from this complex at 300 K.

One might expect that substantial spin–spin coupling occurs between Cu(1) and Cu(2) within the asymmetric unit (type A). Cu(II) ions linked by four syn–syn carboxylate bridges are a feature of the dimeric Cu(II) carboxylate complexes.

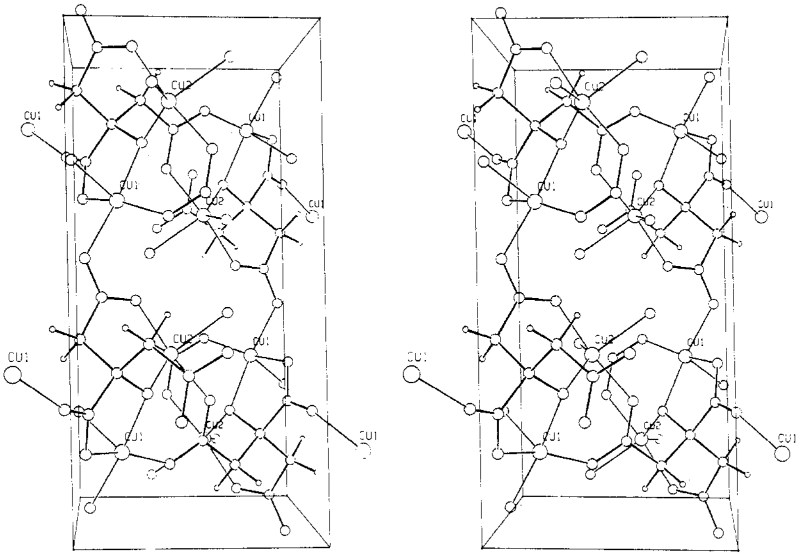

Figure 2. Stereographic view along $\bar{b}$ of the packing of $Cu_2cit \cdot 2H_2O$. The *a* axis is vertical and the *c* axis is horizontal.

Table IV. Weighted Least-Squares Planes

Plane	Atoms defining plane	Equation of mean plane[a]
I	O(7)-O(2)-O(9)-O(3')	$-0.1295X_0 + 0.8451Y_0 - 0.5157Z_0 = 5.444$
II	O(1')-O(5)-O(7)-O(4')	$0.4844X_0 + 0.6306Y_0 - 0.6170Z_0 = 1.261$
III	Cu(2)-O(3')-C(5')-O(4')	$0.1063X_0 + 0.9167Y_0 - 0.3875Z_0 = 6.221$
IV	Cu(2)-O(2)-C(1)-O(1)-Cu(1'')	$-0.0556X_0 - 0.9013Y_0 + 0.4296Z_0 = -6.096$
V	Cu(1)-O(5)-C(6)-O(6)-Cu(1')	$0.5265X_0 - 0.1842Y_0 + 0.8300Z_0 = -2.788$
VI	Cu(1)-Cu(2)-C(3)-O(7)	$-0.3273X_0 - 0.3989Y_0 + 0.8566Z_0 = -0.136$

Displacement of Atoms from Mean Plane, Å

Plane I		Plane II		Plane III		Plane IV		Plane V		Plane VI	
O(7)	−0.37	O(1')	0.20	Cu(2)	0.02	Cu(2)	0.01	Cu(1)	−0.01	Cu(1)	0.00
O(2)	0.36	O(5)	−0.21	O(3')	−0.05	O(2)	−0.21	O(5)	−0.46	Cu(2)	−0.01
O(9)	0.40	O(7)	0.20	C(5')	0.06	C(1)	0.10	C(6)	0.34	C(3)	−0.27
O(3')	−0.39	O(4')	−0.19	O(4')	−0.02	O(1)	0.10	O(6)	0.16	O(7)	0.28
Cu(2)	0.33	Cu(1)	0.14	Cu(1)	−0.56	Cu(1'')	0.03	Cu(1')	−0.02		

Dihedral angle between planes I and II = 38.3°

[a] Equations have the form $AX_0 + BY_0 + CZ_0 = D$ where X_0, Y_0, and Z_0 are Cartesian axes lying along $b \times c^*$, b, and c^*, respectively.

Table V. Magnetochemical Behavior of $Cu_2cit \cdot 2H_2O$[a]

Sample I				Sample II				Sample III			
T, K	$10^6\chi_M$,[b] cgsu	μ,[c] μ_B	μ_{CW},[d] μ_B	T, K	$10^6\chi_M$, cgsu	μ, μ_B	μ_{CW}, μ_B	T, K	$10^6\chi_M$, cgsu	μ, μ_B	μ_{CW}, μ_B
299	1390	1.83	1.75	300	1470	1.88	1.75	299	1510	1.90	1.82
286	1510	1.86	1.78	286	1560	1.89	1.75				
273	1610	1.87	1.79	273	1650	1.90	1.75	273	1680	1.92	1.83
260	1710	1.88	1.80	260	1730	1.90	1.75				
247	1780	1.87	1.78	247	1840	1.90	1.74				
232	1910	1.88	1.79	232	1990	1.92	1.75	232	2000	1.93	1.82
218	2060	1.89	1.79	218	2150	1.93	1.75	218	2140	1.93	1.82
202	2230	1.90	1.79	202	2340	1.94	1.74	202	2320	1.94	1.82
186	2440	1.90	1.78	186	2640	1.98	1.76	186	2590	1.96	1.83
169	2730	1.92	1.78	169	2990	2.01	1.75	169	2890	1.98	1.83
150	3120	1.93	1.78	150	3500	2.05	1.76	150	3330	1.99	1.83
129	3710	1.96	1.77	142	3780	1.97	1.76	129	3980	2.03	1.83
118	4230	2.00	1.76	134	4110	1.97	1.75	118	4310	2.02	1.80
106	4940	2.05	1.81	125	4480	1.95	1.75	106	5050	2.07	1.82
96	5520	2.06	1.79	116	4950	1.95	1.74	93	5910	2.10	1.81
85	6150	2.04	1.75	106	5420	1.92	1.69				

[a] Cu(II):citric acid:urea ratios of 2:1:2 were used to prepare samples I and II; a ratio of 1:1:1.5 was used to prepare sample III. [b] The molar susceptibility χ_M is *per* Cu(II) and includes a diamagnetic correction of 74×10^{-6} cgsu. [c] $\mu = (7.998\chi_M T)^{1/2}$. [d] $\mu_{CW} = [7.998\chi_M \cdot (T - \Theta)]^{1/2}$; Θ's for samples I, II, and III are +25 ± 4, +40 ± 4, and +24 ± 4 K, respectively.

Such complexes exhibit substantial antiferromagnetism with magnetic moments per Cu(II) of ~1.4 μ_B at 300 K.[17] A recent study indicates that Cu(II) ions linked by two syn–syn carboxylate bridges may exhibit comparable antiferromagnetism, although this inference is weakened by the presence of a second type of bridging.[18] The magnetic consequence of Cu(1) lying 0.56 Å below the O(3')–C(5')–O(4')–Cu(2) fragment in the citrate structure is difficult to

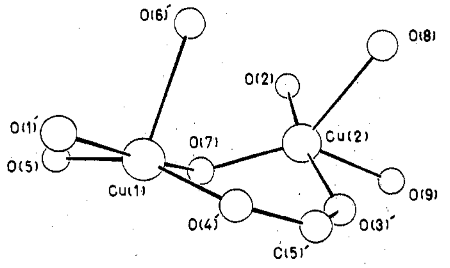

Figure 3. Relative orientations of the Cu(1) and Cu(2) coordination spheres.

quantify but probably leads to reduced spin–spin coupling relative to that of a fully planar system. On the basis of the reported magnetic behavior of $Cu_2(OH)_2^{2+}$ and $Cu_2(OR)_2^{2+}$ structural species,[2,19,20] the alkoxo bridge in the citrate structure might also be expected to result in substantial antiferromagnetism. Furthermore, the reported variation of spin–spin coupling with the bridging angle of $Cu_2(OH)_2^{4+}$ systems indicates that the bent (115°) alkoxo bridge in the citrate structure should allow particularly effective coupling.[2] The observed net magnetic behavior indicates either that the anticipated antiferromagnetic coupling between Cu(1) and Cu(2) within the asymmetric unit is overcome by ferromagnetic coupling along and/or between the chains or that coupling via the alkoxo and syn–syn carboxylate links is unexpectedly small. We believe this latter result is most likely. Strong antiferromagnetic coupling within the dimeric copper(II) carboxylate and $Cu_2(OH)_2^{4+}$ units is associated with a characteristic absorption band at ~380 nm not exhibited by magnetically dilute Cu(II) reference complexes.[19,21] The reflectance spectra of $Cu_2cit{\cdot}2H_2O$ at 300 K consist of a broad d–d absorption centered at ~775 nm along with the usual carboxylate → Cu(II) charge-transfer band at ~250 nm. There is no indication of the "extra" absorption band associated with strongly coupled oxygen-bridged Cu(II) dimers. Presumably, coupling via the syn–syn carboxylate bridge has been seriously reduced by the noncoplanarity of this unit (vide supra). Also, it appears that the twist between the coordination spheres of Cu(1) and Cu(2) (Table IV) has reduced the ability of the alkoxo bridge to couple Cu(1) and Cu(2) magnetically.

Finally, the reported magnetic[22] (weak ferromagnetism) and structural[23] studies of the royal blue modification of copper formate support the inference that spin–spin coupling via the anti–syn B and C type bridges is not strongly ferromagnetic. The structure of $Cu(HCO_2)_2$ consists of a three-dimensional array of Cu(II) ions linked primarily by anti–syn formate bridging to all four equatorial positions. An additional apical bond results in five-coordination.

Acknowledgment. This research was supported by the Rutgers Computing Center and in part by a grant (AM16412) from the National Institutes of Health. Magnetic measurements were made in the laboratory of Professor Harry B. Gray at the California Institute of Technology; H.J.S. thanks Professor Gray for his hospitality.

Registry No. $Cu_2C_6H_4O_7{\cdot}2H_2O$, 58846-97-2.

Supplementary Material Available: Listing of structure factor amplitudes (6 pages). Ordering information is given on any current masthead page.

References and Notes

(1) R. H. Dunhill, J. R. Pilbrow, and T. D. Smith, *J. Chem. Phys.*, **45**, 1474 (1966), and references therein.
(2) K. T. McGregor, N. T. Watkins, D. L. Lewis, R. F. Drake, D. J. Hodgson, and W. E. Hatfield, *Inorg. Nucl. Chem. Lett.*, **9**, 423 (1973).
(3) R. W. Parry and F. W. DuBois, *J. Am. Chem. Soc.*, **74**, 3749 (1952).
(4) H. J. Schugar, G. R. Rossman, C. G. Barraclough, and H. B. Gray, *J. Am. Chem. Soc.*, **94**, 2683 (1972).
(5) A. Earnshaw, "Introduction to Magnetochemistry", Academic Press, New York, N.Y., 1968.
(6) B. W. Low and F. M. Richards, *J. Am. Chem. Soc.*, **74**, 1660 (1952).
(7) R. C. Weast, Ed., "Handbook of Chemistry and Physics", 46th ed, Chemical Rubber Publishing Co., Cleveland, Ohio.
(8) In addition to local programs for the IBM 360/67 computer, locally modified versions of the following programs were employed: Zalkin's FORDAP Fourier program; Johnson's ORTEP II thermal ellipsoid plotting program; the ORFFE error function and ORFLS least-squares programs of Busing, Martin, and Levy. The analysis of variance was carried out using program NANOVA obtained from Professor I. Bernal; see J. S. Ricci, Jr., C. A. Eggers, and I. Bernal, *Inorg. Chim. Acta*, **6**, 97 (1972).
(9) D. T. Cromer and J. T. Waber, *Acta Crystallogr.*, **18**, 104 (1965).
(10) "International Tables for X-Ray Crystallography", Vol. III, Kynoch Press, Birmingham, England, 1962, pp 201–216.
(11) Supplementary material.
(12) J. Fischer and R. Weiss, *Acta Crystallogr., Sect. B*, **29**, 1963 (1973).
(13) K. Nakamoto, "Infrared Spectra of Inorganic and Coordination Compounds", Wiley-Interscience, New York, N.Y., 1970.
(14) C. K. Johnson, *Acta Crystallogr.*, **18**, 1004 (1965).
(15) J. P. Glusker and H. L. Carrell, *J. Mol. Struct.*, **15**, 151 (1973).
(16) B. Sheldrick, *Acta Crystallogr., Sect. B*, **30**, 2056 (1974).
(17) M. Kato, H. B. Jonassen, and J. C. Fanning, *Chem. Rev.*, **64**, 99 (1964).
(18) D. B. W. Yawney and R. J. Doedens, *J. Am. Chem. Soc.*, **92**, 6350 (1970).
(19) Y. Nishida, F. Numata, and S. Kida, *Inorg. Chim. Acta*, **11**, 189 (1974).
(20) J. A. Bertrand and R. I. Kaplan, *Inorg. Chem.*, **4**, 1657 (1965).
(21) H. J. Schugar, E. I. Solomon, W. L. Cleveland, and L. Goodman, *J. Am. Chem. Soc.*, **97**, 6442 (1975).
(22) M. Inoue and M. Kubo, *Inorg. Chem.*, **9**, 2310 (1970).
(23) G. A. Barclay and C. H. L. Kennard, *J. Chem. Soc.*, 3289 (1961).

Notes

Contribution from the Department of Chemistry,
University of Georgia, Athens, Georgia 30602,
and the Office of Naval Research,
Arlington, Virginia 22217

Chalocogen Chemistry. 10. Synthesis and Characterization of Triarylphosphine Adducts of Selenium(II) Bromide

Daniel J. Williams and Kenneth J. Wynne*

Received July 29, 1975 AIC50561T

There have recently been reported compounds of the general type $SeBr_2(Z)$ where Z is a two-electron donor. One example is $SeBr_2$tmtu (Z = tmtu, 1,1,3,3-tetramethyl-2-thiourea),[1] which is prepared either through the reaction of $SeBr_4$ with excess tmtu in CH_2Cl_2 or through reaction of $RSeBr_3$ (R = CH_3, CH_3CH_2) and tmtu. $SeBr_2$tmtu is a red crystalline solid stable to atmospheric moisture. T-shaped $SeBr_2$tmtu units loosely joined via halogen bridges exist in the crystal.

Salts containing the $C_6H_5SeBr_2^-$ anion ($Z = C_6H_5^-$)[2] and the $SeCNBr_2^-$ anion ($Z = CN^-$)[3] are also known. The former is prepared through the reaction of a tetraalkylammonium bromide with phenylselenyl bromide, and the latter is prepared through the reaction of bromine with tetraalkylammonium selenocyanates. This work reports our attempts to extend knowledge of selenium(II) chemistry to include triarylphosphines as the two-electron donor, Z.

Experimental Section

Due to the moisture sensitivity of the compounds involved, all work was done in polyethylene glovebags under a dry nitrogen atmosphere.

---

* To whom correspondence should be addressed at the office of Naval Research.